Cloaking: Controlling Thermal and Hydrodynamic Fields Simultaneously

Woon-Shing Yeung,[†] Van-Phung Mai, and Ruey-Jen Yang[*]
Department of Engineering Science, National Cheng Kung University, Tainan, Taiwan

(Received 10 January 2020; revised manuscript received 16 April 2020; accepted 6 May 2020; published 12 June 2020)

Hydrodynamic and thermal cloaking effects have attracted interest among researchers using metamaterials. This paper explores an analytical solution using only isotropic materials to achieve cloaking under forced convective heat transfer. It is shown that, under a background of uniform flow and linearly varying temperature, a circular bilayer cloak with an inner layer made of impenetrable and insulated material and an outer layer made of a porous medium having a constant permeability and effective conductivity does not disturb the external flow and temperature fields. Moreover, the cloaked region is shielded from the external flow and temperature fields. Analytical temperature and velocity distributions within the porous outer layer are presented to demonstrate both the hydrodynamic and thermal cloaking effects of such a bilayer. Finally, numerical results, based on practically attainable material properties, are given to confirm the analytical model.

DOI: 10.1103/PhysRevApplied.13.064030

I. INTRODUCTION

Thermal cloaking under pure conduction heat transfer has been well studied in recent years. Two main methodologies have been put forth: transformation thermodynamics (e.g., [1]) and bilayer theory [2]. Transformation thermodynamics leads to the concept of thermal metamaterials having relatively complicated nonhomogeneous and anisotropic thermal conductivity. On the other hand, the bilayer theory yields a thermal cloak design relying only on natural bulk materials. Only relatively recently has thermal cloaking under forced convective heat transfer conditions started to attract interest among researchers. Unlike cloaking under pure conduction, cloaking under convection involves also fluid flow. Therefore, cloaking under a convective background must not disturb either the thermal or the hydrodynamic field of the background. Such a cloak not only provides thermal protection for the cloaked object, but also hydrodynamic protection (such as drag reduction).

A systematic study of a cloak under convective conditions has been conducted by Dai *et al.* [3] for steady flow and Dai and Huang [4] for transient flow, following the precepts of transformation thermodynamics. Under the situation of creeping flow in porous media, it is shown that Darcy's law and the convection-diffusion energy equation are form-invariant under coordinate transformation [3]. The transformed permeability and effective conductivity of the porous cloak depend on the Jacobian of transformation as in the conduction case. Numerical simulation demonstrates the full cloaking ability of the proposed cloak [3]. As in the case of conduction thermal cloaking, construction of a cloak having the required transformed properties is a challenge. In contrast, the bilayer theory does not rely on transformation thermodynamics, and is much simpler in application [2].

The present study is motivated by the bilayer theory. Specifically, we explore the possibility of finding a bilayer cloak, made of isotropic media, which functions in a convective background. The present analysis considers the same physical system as in Dai *et al.* [3], corresponding to a circular cloak subject to a background of uniform velocity in either the horizontal or vertical direction, and a temperature field governed by a high and low temperature at the left and right side of the background region respectively. Two situations were considered in Dai *et al.* [3]: one corresponds to the flow direction being parallel and the other to the flow direction being perpendicular to the heat flux direction. The perpendicular case is the one studied here, since the background temperature field can be shown to be linear as in the common conduction thermal cloaking situation studied by most researchers. The parallel case yields a nonlinear temperature distribution (due to the advection term in the energy equation) and therefore may not be amenable to an analytical solution for the bilayer design.

Our study is based on creeping flow in porous media as in Dai *et al.* [3] and Urzhumov and Smith [5]. Recently, hydrodynamic metamaterials of microfluidic structures have been proposed by Park *et al.* [6,7] for hydrodynamic cloaking. Application to flow stabilization and wake reduction is also proposed in Urzhumov and Smith [8] and Culver and Urzhumov [9], respectively.

[*]rjyang@mail.ncku.edu.tw
[†]Visiting scientist from the University of Massachusetts, Lowell, MA.

II. THEORY

Figure 1 shows the notations of the physical system under consideration. A bilayer cloak is centrally located in a square region of $a \times a$ as shown. As for the conduction bilayer cloak, the cloaked region is defined by $r < R_0$, the inner layer $R_0 \leq r < R_1$, and the porous outer layer $R_1 \leq r < R_2$. The background is defined by $r \geq R_2$. r and θ denote the polar coordinates. The various regions depicted in Fig. 1 are background (region 4), outer layer (region 3), inner layer (region 2), and cloaked region (region 1). In the conduction bilayer theory, the inner layer is perfectly insulated and the outer layer has a specific conductivity depending on the dimensions of outer layer (i.e., R_1 and R_2). A uniform velocity flow field is imposed in the y direction (vertical) by means of a prescribed high and low pressure at the bottom and top boundary, respectively, and the left and right sides are subject to a high and low temperature, respectively. Thus, the background velocity is described by

$$u = 0, \tag{1}$$

$$v = v_\infty, \tag{2}$$

where u and v are the velocity components, respectively, in the x and y directions and v_∞ is the imposed uniform velocity. Note that this background velocity applies in the domain $r > R_2$; otherwise the cloak would fail to provide the necessary cloaking function for the hydrodynamic field.

A. Thermal consideration

Consider the thermal field first. The steady-state energy equation for incompressible flow without heat sources and negligible viscous dissipation in the background is given by the advection-diffusion equation (e.g., [10]) as follows:

$$\rho_f C_{\mathrm{pf}} \left(u\frac{\partial T}{\partial x} + v\frac{\partial T}{\partial y} \right) = k_f \left(\frac{\partial^2 T}{\partial x^2} + \frac{\partial^2 T}{\partial y^2} \right), \tag{3}$$

where ρ_f is the fluid density, C_{pf} is the fluid specific heat, k_f is the fluid conductivity, and T is the fluid temperature. For the particular flow and thermal field arrangement considered here, the advection term is approximately zero since $u = 0$, and temperature varies mainly in the x direction. Hence

$$\frac{\partial^2 T}{\partial x^2} = 0, \tag{4}$$

subject to the following boundary conditions:

$$T = T_H \text{ at } x = -a/2, \quad T = T_L \text{ at } x = a/2. \tag{5}$$

The resulting background temperature is therefore linear in x with a constant gradient, t_0, given by $(T_L - T_H)/a$.

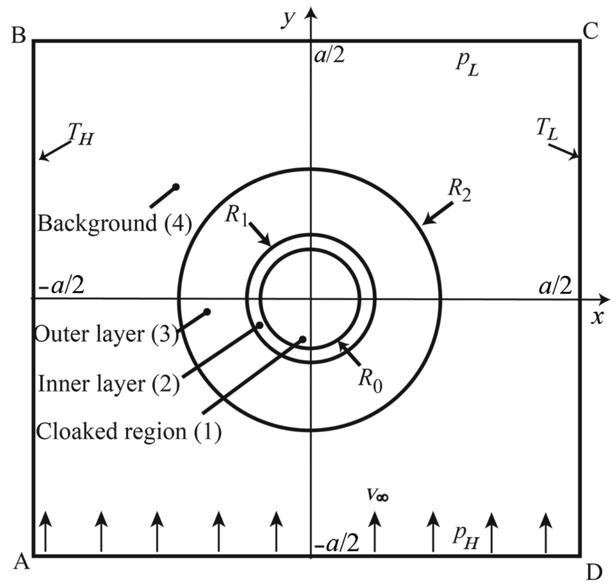

FIG. 1. Schematic of bilayer convection cloak. The domain of interest is denoted by ABCD with the origin at the center of the domain. Constant temperature T_H and T_L are prescribed on AB and DC, respectively, with AD and BC insulated. Constant pressure p_H and p_L are prescribed on AD and BC, respectively.

The temperature in the porous outer layer is also governed by the advection-diffusion equation, Eq. (3). Note that both u and v are nonzero within the outer layer, such that the argument used for the background does not apply to the outer layer. However, for small Péclet number, $\mathrm{Pe} = \mathrm{PrRe} \ll 1$ (Pr is the Prandtl number, $C_{\mathrm{pf}}\mu_f/k_3$, and Re is the Reynolds number, $\rho_f v_\infty R_2/\mu_f$, with R_2 taken as the characteristic length of the system, μ_f as the fluid dynamic viscosity, and k_3 an effective conductivity of the porous medium), the advection term can be neglected (e.g., [11]) and the temperature in the porous outer layer is then governed by the Laplace equation as in the conduction case. The result of Ref. [2] therefore applies to temperature cloaking:

$$\frac{k_3}{k_4} = \frac{R_1^2 + R_2^2}{R_2^2 - R_1^2}, \tag{6}$$

where k_3 and k_4 are, respectively, the conductivity of the outer layer and background [2]. The derivation of Eq. (6) is worth mentioning. Note that the supplemental material [12] of Han *et al.* [2] contains a detailed derivation for the three-dimensional case. Following the same steps as outlined in Ref. [12], the temperature distribution, relative to an average temperature $T_{\mathrm{avg}} = (T_H + T_L)/2$, for the various regions depicted in Fig. 1 is given by a Fourier series similar to Eq. (17) given later in the hydrodynamic consideration (Sec. II B), i.e.,

$$T_i = \sum_{t=1}^{\infty} \left[\zeta_{t,i} r + \eta_{t,i}/r\right] (\cos t\theta + \sin t\theta), \tag{7}$$

where i denotes the region and $\zeta_{t,i}$ and $\eta_{t,i}$ are constants to be determined by interface conditions at $r = R_2$ and $r = R_1$ (i.e., continuity in temperature and normal heat flux). Since the background temperature is linear in x, only the $t = 1$ cosine term is required in Eq. (7). Stipulating that the background temperature field must not be disturbed, and that the inner layer is perfectly insulated (i.e., $k_1 = 0$), one can solve for the constants $\zeta_{t,i}$ and $\eta_{t,i}$, and thus arrive at Eq. (6) above. In particular, it can be shown that

$$\zeta_{1,3} = \eta_{1,3}/R_1^2 \quad \text{and} \quad \eta_{1,3} = t_0 R_2^2/(1 + R_2^2/R_1^2) \tag{8}$$

for the outer layer.

Note that for convection cloaking, k_3 is the effective conductivity for a porous medium. The background conductivity, k_4, is either the fluid conductivity, k_f, if the background is a normal fluid medium or an effective conductivity if the background is also a porous medium. The effective conductivity of a porous medium is given by

$$k_3 = k_s(1 - \phi) + \phi k_f, \tag{9}$$

where ϕ is the so-called porosity of the porous medium and k_s is the conductivity of the solid material making up the porous medium. Knowing the effective conductivity from Eq. (6), the porosity of the porous medium can be calculated from Eq. (9), given k_s and k_f.

The corresponding temperature field in the porous outer layer, which can be inferred from Ref. [12], can now be obtained from Eqs. (7) and (8) as follows:

$$T_3 = \frac{t_0 R_2^2}{1 + R_2^2/R_1^2} \left(\frac{r}{R_1^2} + \frac{1}{r}\right) \cos\theta, \tag{10}$$

where t_0 is the constant temperature gradient defined earlier. Recall that the temperature is relative to the average temperature T_{avg}; hence the actual temperature is given by $T_3 + T_{\text{avg}}$.

B. Hydrodynamic consideration

Next, consider the hydrodynamic field. In the analysis of Dai *et al.* [3], the background is also assumed as a porous medium having an isotropic permeability. Under creeping flow (Re $\ll 1$) and small permeability ($K \ll R_2^2$), Darcy's law applies (note that Darcy's law also applies to media with anisotropic permeability); see Bear [10]. Accordingly, the constant velocity field can be realized by applying a constant pressure gradient in the flow direction. It is thus similar to Problem A considered in Urzhumov and Smith [5]. Retaining the same assumption as in Dai *et al.* [3], we can proceed as follows. Darcy's law for the background is given by

$$\vec{\nabla} p + \frac{\mu_f}{K_4} \vec{v} = 0, \tag{11}$$

where K_4 is the permeability of the background. Since the postulated velocity in the background is uniform and in the y direction only, the background pressure field is then

$$(dp_4/dy) = -\mu_f v_\infty / K_4 = p_0', \tag{12}$$

subject to the following boundary conditions:

$$p_4 = p_H \text{ at } y = -a/2, \quad p_4 = p_L \text{ at } y = a/2. \tag{13}$$

The resulting background pressure is therefore linear in y with a constant pressure gradient p_0', given by $(p_L - p_H)/a$.

For the outer layer, Darcy's law can be written as

$$\vec{\nabla} p + \frac{\mu_f}{K_3} \vec{v} = 0. \tag{14}$$

The continuity equation is given by

$$\vec{\nabla} \cdot \vec{v} = 0. \tag{15}$$

Combining Darcy's law and the continuity equation, one obtains

$$\nabla^2 p = 0. \tag{16}$$

The above derivation inspires the present study, and supports the possibility of a bilayer convection cloak. In the bilayer theory for conduction, the temperature field satisfies the Laplace equation, and the background is characterized by a constant temperature gradient. In the present case, the pressure field satisfies the Laplace equation, and the background is characterized by a constant pressure gradient, p_0'. Thus pressure in the convection cloak assumes the role of temperature in the conduction cloak, and the same analysis as in the bilayer theory may be applied here. Proceeding as in the thermal consideration, the general solution (in polar coordinates r and θ) for the pressure field, relative to an average pressure $p_{\text{avg}} = (p_H + p_L)/2$, is then

$$p_i = \sum_{t=1}^{\infty} \left[\alpha_{t,i} r + \beta_{t,i}/r\right] (\cos t\theta + \sin t\theta), \tag{17}$$

where i denotes the region and $\alpha_{t,i}$ and $\beta_{t,i}$ are constants to be determined by boundary and interface conditions. For a convection cloak, only $i = 4$ (background) and $i = 3$ (outer layer) need to be considered, for pressure. The inner layer, as usual, is an insulated layer (for thermal cloaking) and impenetrable (for hydrodynamic cloaking). The main question is then: what is the permeability of the porous outer layer such that the pressure and velocity fields in the background are not disturbed?

As usual, for a linear pressure gradient field in the background (in the y direction), p_4 is given by

$$p_4 = p_0' r \sin\theta. \tag{18}$$

Therefore, only the $t = 1$ sine term is needed in the general solution. In addition, $\beta_{1,4} = 0$ and $\alpha_{1,4} = p_0'$. The pressure field in the porous outer shell is

$$p_3 = (\alpha_{1,3} r + \beta_{1,3}/r)\sin\theta. \tag{19}$$

As for a conduction bilayer cloak, the unknown coefficients in the general solution are determined by interface conditions. For convection cloaking, the interface conditions are as follows:

1. Pressure is continuous at the outer boundary of the outer layer: $p_3|_{R_2} = p_4|_{R_2}$.
2. There is mass continuity at the outer boundary of the outer layer. Note that mass continuity only requires normal velocity, not tangential velocity, be continuous at the interface between the background and the outer layer: $(v_3)_r|_{R_2} = (v_4)_r|_{R_2}$, where the subscript r denotes the radial component of the velocity vector.
3. Normal velocity is zero at the interface between the outer layer (porous) and inner layer (impervious); e.g., see Sec. 5.2.4 of Bear [10]. Hence $(v_3)_r|_{R_1} = 0$.

The first interface condition yields

$$\alpha_{1,3} R_2 + \beta_{1,3}/R_2 = p_0' R_2. \tag{20}$$

The velocity in the porous shell can now be evaluated from Eqs. (14) and (19). In cylindrical polar coordinates, the velocity components in the porous layer can be shown to be (see Ref. [13] for a general discussion of curvilinear coordinates)

$$(v_3)_r = -\frac{K_3}{\mu_f}\left(\alpha_{1,3} - \frac{\beta_{1,3}}{r^2}\right)\sin\theta, \tag{21}$$

$$(v_3)_\theta = -\frac{K_3}{\mu_f}\left(\alpha_{1,3} + \frac{\beta_{1,3}}{r^2}\right)\cos\theta. \tag{22}$$

Applying the second interface condition at $r = R_2$, one gets another equation relating $\alpha_{1,3}$ and $\beta_{1,3}$:

$$-\frac{K_3}{\mu_f}\left(\alpha_{1,3} - \frac{\beta_{1,3}}{R_2^2}\right) = v_\infty, \tag{23}$$

since $(v_4)_r = v_\infty \sin\theta$ at $r = R_2$. Finally, applying the third interface condition at the interface between the outer and inner shell, i.e., at $r = R_1$, and for nonzero K_3, we have

$$\alpha_{1,3} = \beta_{1,3}/R_1^2. \tag{24}$$

Equations (24) and (20) determine $\alpha_{1,3}$ and $\beta_{1,3}$. The results are

$$\alpha_{1,3} = \frac{p_0' R_2^2/R_1^2}{1 + R_2^2/R_1^2}, \quad \beta_{1,3} = \frac{R_2^2 p_0'}{1 + R_2^2/R_1^2}. \tag{25}$$

The pressure in the outer layer is then given by, from Eqs. (19) and (25),

$$p_3 = \frac{p_0' R_2^2}{1 + R_2^2/R_1^2}\left(\frac{r}{R_1^2} + \frac{1}{r}\right)\sin\theta. \tag{26}$$

As for temperature, recall that the pressure is relative to the average pressure p_{avg}; hence the actual pressure is given by $p_3 + p_{\text{avg}}$.

Using $\alpha_{1,3}$ and $\beta_{1,3}$ in Eq. (23), K_3 can be derived as

$$K_3 = -\frac{(R_1^2 + R_2^2) v_\infty \mu_f}{p_0'(R_2^2 - R_1^2)}. \tag{27}$$

Note that since the pressure gradient is negative, the resulting K_3 is positive as physically expected. The quantity $-v_\infty \mu_f / p_0'$ in Eq. (27) is simply K_4 from Eq. (12). Hence Eq. (27) can be rewritten as

$$\frac{K_3}{K_4} = \frac{(R_2^2 + R_1^2)}{(R_2^2 - R_1^2)}, \tag{28}$$

which is exactly the same as the conductivity ratio for the bilayer theory [Eq. (6)]. That the conductivity and permeability ratio between the outer shell and the background is governed by the same geometric relation is quite surprising, since they are derived under seemingly different interfacial conditions. Further examination of our formulation reveals that Darcy's law, Eq. (14), and the Fourier law of heat conduction are of the same form, if one replaces pressure with temperature, velocity with heat flux, and K_3/μ_f with conductivity. Thus streamlines governed by Darcy's law are equivalent to heat flux lines governed by the Fourier law. This perspective conclusively verifies the hydrodynamic cloaking function of our proposed bilayer cloak. Physically, K_4 can be interpreted as the resistance that the pressure gradient must overcome in order to produce a uniform flow of v_∞ in a fluid with dynamic viscosity μ_f.

To recap, a convection bilayer cloak could be realized by using an isotropic porous outer shell having an effective conductivity given by Eq. (6) and permeability given by Eq. (28), and an impenetrable inner shell of zero conductivity. Such a cloak will preserve both the background temperature and velocity field. In particular, the background temperature remains linear in the x direction and the background velocity uniform in the y direction.

III. ANALYTICAL RESULTS

Before proceeding to numerical simulation, we give here the analytical results based on the model equations derived above. Consider the following example. $R_2 = 2R_1 = 20$ μm, $a = 80$ μm, $T_H = 303$ K, and $T_L = 293$ K. The background material (assumed porous in this study) is characterized by $\rho_f = 10^3$ kg/m^3, $C_{\mathrm{pf}} = 5 \times 10^3$ J/kg K, $k_4 = 10$ W/m K, $\mu_f = 10^{-3}$ Pa s, and $K_4 = 10^{-12}$ m^2 (corresponds to approximately 1 darcy in permeability). The applied pressure difference is 400 Pa (i.e., $p_H = 400$ Pa, $p_L = 0$ Pa), such that the pressure gradient is $p_0' = -\Delta p/a = -5 \times 10^6$ Pa/m. The resulting background speed is then, from Eq. (12), $-p_0' K_4/\mu_f$ or 5×10^{-3} m/s. The inner layer (not present in Dai *et al.* [3]) is arbitrarily assigned a radius of $R_0 = 8$ μm. The above is the same case considered in Dai *et al.* [3], except for k_4, which is explicitly specified here. The relatively high k_4 value chosen is to better satisfy the assumption that conduction is dominant over advection in the background and in the porous outer layer. Note that the analytical solution derived herein is independent of k_s, k_f, and porosity ϕ of the porous media. The porosity of either the background or the porous outer layer can be determined for a combination of k_s and k_f values, once the effective conductivity is known. For the present numerical example, the required effective conductivity of the outer layer as calculated from Eq. (6) is 16.67 W/m K. The required permeability of the porous outer layer as calculated from Eq. (28) is 1.67×10^{-12} m^2. For this example, the Reynolds number is calculated as 0.1 and the Péclet number is approximately 0.03. Moreover, K_3/R_2^2 is approximately 0.004. Thus, the validity of Darcy's law and the Laplace equation for the outer layer is confirmed.

Consider first the thermal field. Figure 2 shows the isotherms in the outer layer (top half), based on Eq. (10). These isotherms are the typical isotherms in a conduction bilayer cloak as given in Han *et al.* [2]. Next consider the flow field. Figure 3 shows the isobars (lines of constant pressure, right half), based on Eq. (19). As seen, they are similar to the isotherms since the pressure in a porous medium satisfying Darcy's law is governed by the Laplace equation. The streamlines can be expressed symbolically as

$$dy/dx = v_y/v_x, \tag{29}$$

where v_x and v_y are the x and y components of the velocity vector inside the porous outer layer, and can be obtained from the r and θ components, Eqs. (21) and (22), respectively, as follows:

$$v_x = v_r \cos\theta - v_\theta \sin\theta, \tag{30}$$

$$v_y = v_r \sin\theta + v_\theta \cos\theta. \tag{31}$$

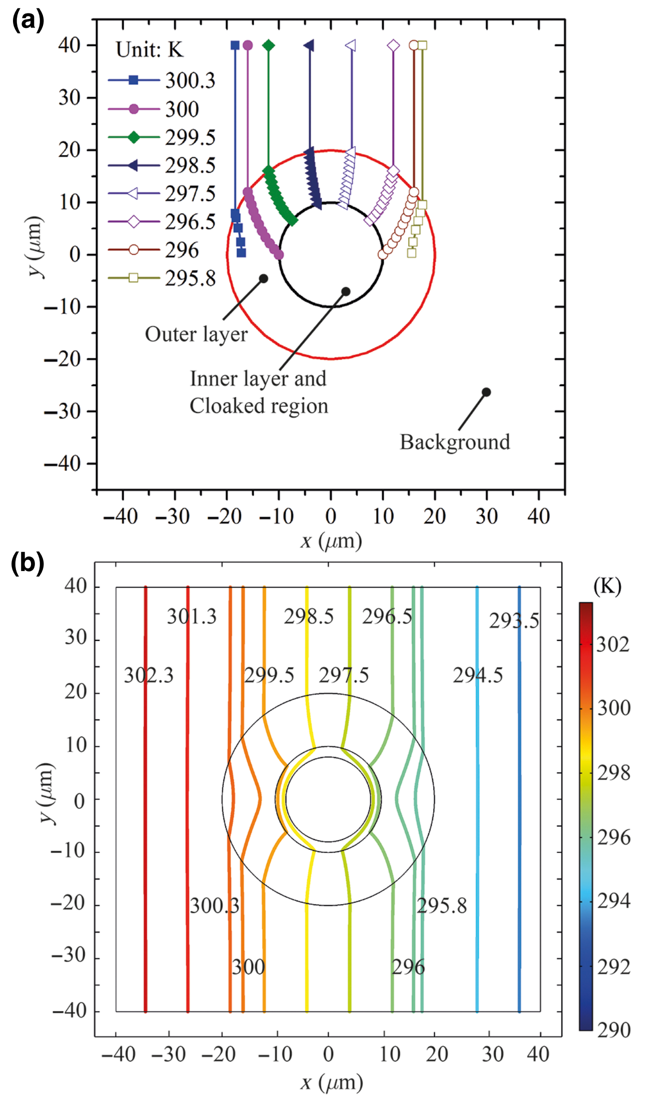

FIG. 2. Isotherms in the outer layer of the convection cloak. (a) Analytical. The analytical results are obtained by setting T_3 in Eq. (10) to the indicated values inside the outer layer ($R_1 < r < R_2$). In the background ($r > R_2$), the isotherms are simply vertical lines for a linear background temperature field. (b) COMSOL.

For instance, in the background, v_x is zero. Hence dy/dx is ∞ and the streamlines are vertical (see Fig. 4).

IV. NUMERICAL SIMULATION

To further demonstrate the functionality of the proposed bilayer convection cloak, and to assess the validity of the assumptions, numerical simulation using the COMSOL MULTIPHYSICS code is conducted using two templates: full advection-diffusion equation [Eq. (3)] and Darcy's law [Eqs. (14) and (11)]. Since the full energy equation is used, the validity of the assumption regarding conduction dominance can be verified in both the background and outer-layer region.

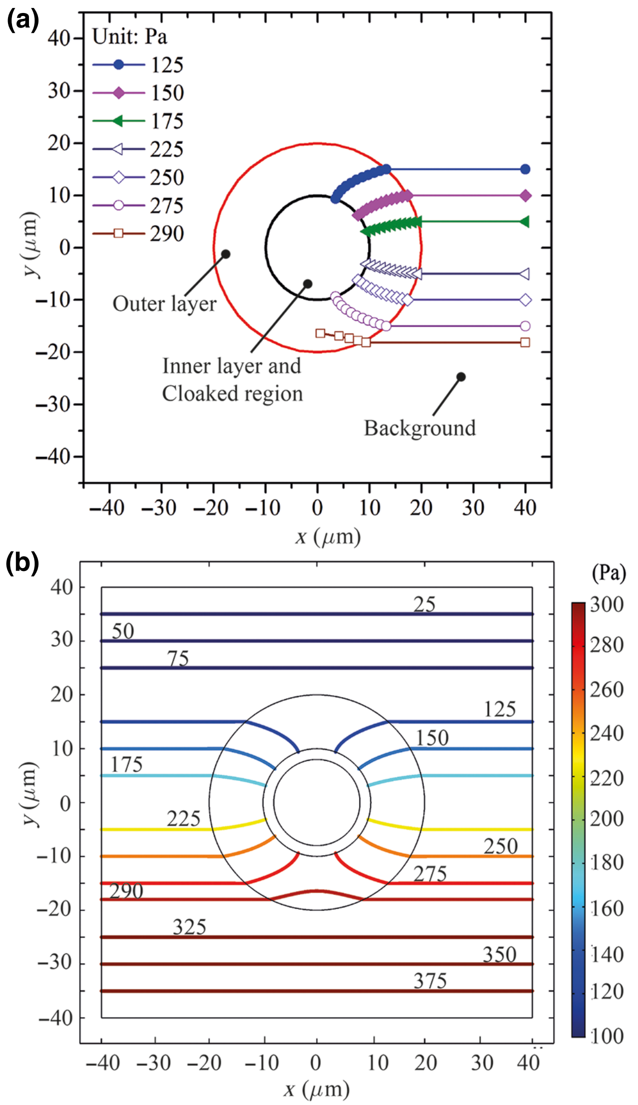

FIG. 3. Isobars in the outer layer of the convection cloak. (a) Analytical. The analytical results are obtained by setting p_3 in Eq. (19) to the indicated values inside the outer layer ($R_1 < r < R_2$). In the background ($r > R_2$), the isobars are simply horizontal lines for a linear background pressure field. (b) COMSOL.

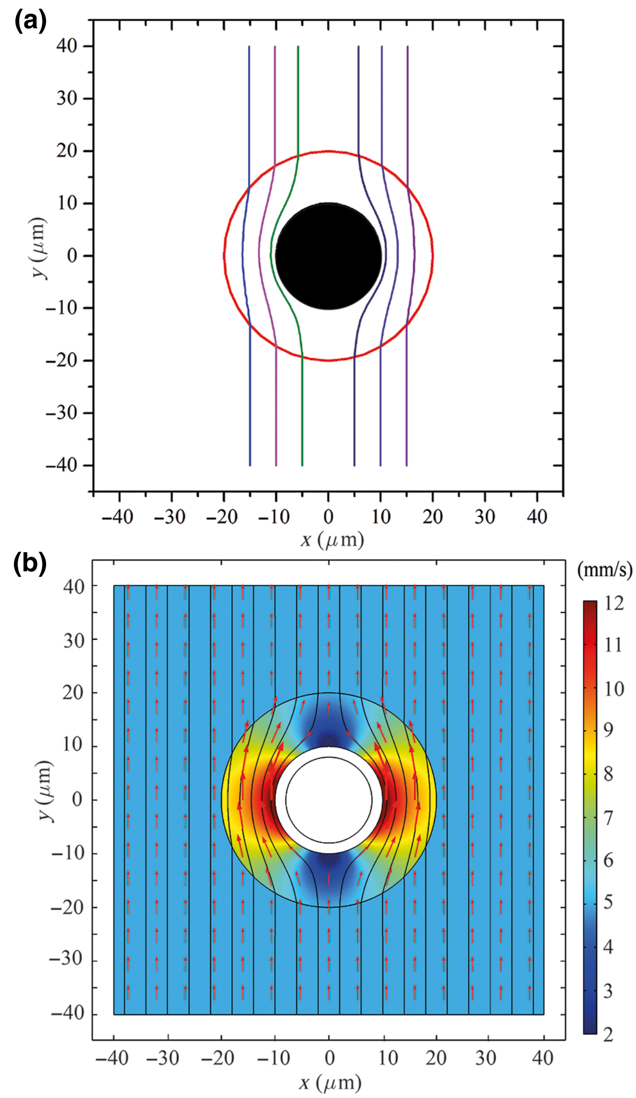

FIG. 4. Streamlines in the background and outer layer. (a) Analytical. The analytical streamlines are obtained by numerically integrating Eq. (29) from a position starting from the lower boundary. (b) COMSOL. Velocity vectors are shown in red arrows, with magnitudes indicated by the color bar on the right.

The domain of computation is the square ABCD as shown in Fig. 1. The adaptive meshing scheme in COMSOL is used, with fine meshing of quadrilateral elements in the vicinity of both interfaces ($r = R_1$ and $r = R_2$) and regular meshing of triangular elements elsewhere. All simulations use the steady-state solver option in COMSOL. A mesh study is first performed and it is determined that a mesh consisting of 36 000 elements is adequate to give converged results. The thermal boundary conditions applied consist of constant temperature T_H and T_L on AB and DC, respectively, and insulated condition on AD and BC. The hydrodynamic boundary conditions applied consist of constant pressure p_H and p_L on AD and BC, respectively, and zero normal flow on AB and DC. Porous medium is selected for both background and outer layer, and solid medium for both inner and cloaked region. Material properties as specified in the analytical solutions (Sec. III) are assigned to each region. For simulation purposes, the cloaked region ($r < R_0$) is given the following properties: density 10^4 kg/m^3, specific heat 5000 J/kg K, and conductivity 200 W/m K. Also, the inner layer is assigned a conductivity of 0.15 W/m K corresponding to the material polydimethylsiloxane (PDMS). As mentioned in the analytical solutions, our analysis is independent of porosity; hence arbitrary porosities of 0.97 and 1.0 are assigned for

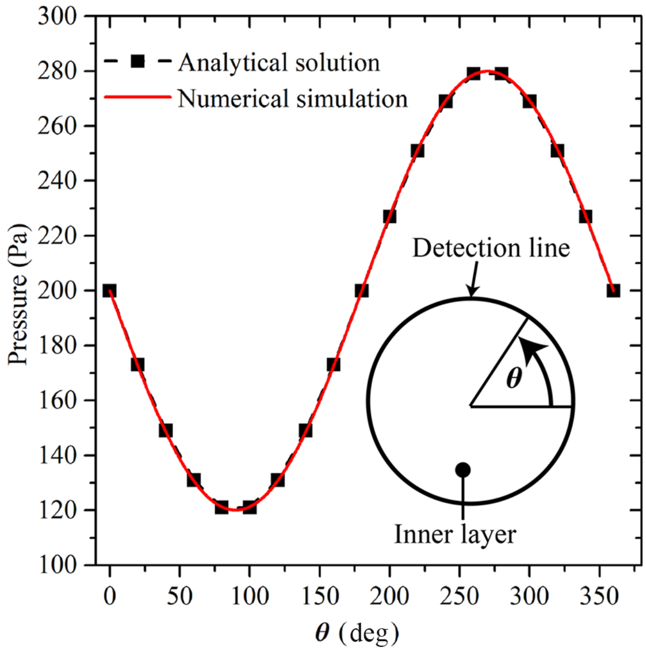

FIG. 5. Pressure distribution on the outer radius of the inner layer of the convection cloak.

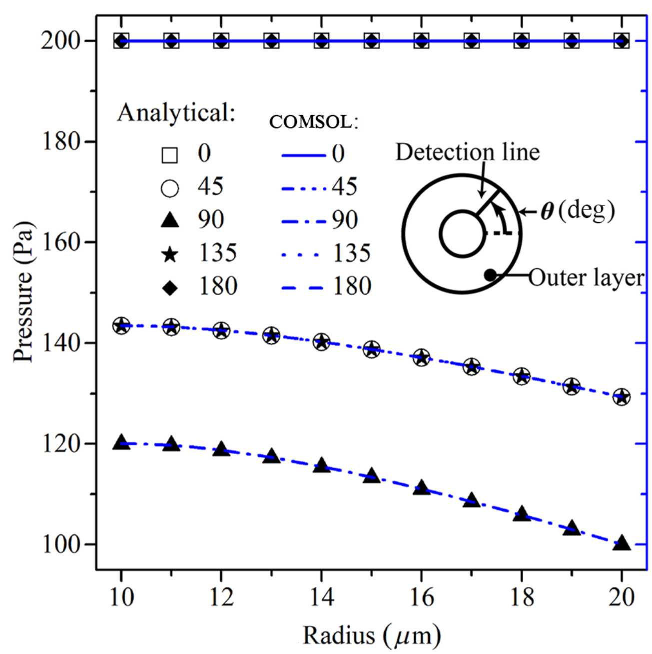

FIG. 7. Comparison of pressure distribution in outer layer.

the outer layer and background, respectively. Realistic values of k_f and k_s can be specified to give other porosity values as necessary.

The COMSOL isotherms, isobars, and streamlines are shown together with the analytical results in Figs. 2–4, respectively. As seen, the isotherms are the same as the analytical isotherms, verifying that the assumption of dominant conduction in the background and the outer layer is valid (since the analytical isotherms are based on the Laplace equation of heat conduction) for the case simulated.

Additional comparisons with the analytical results are given as follows. Figure 5 shows the pressure distribution on the outer radius of the inner layer (i.e., at $r = R_1$) and comparison to the analytical results [Eq. (10)] at $r = R_1$. Excellent agreement is obtained. Figures 6 and 7 show the

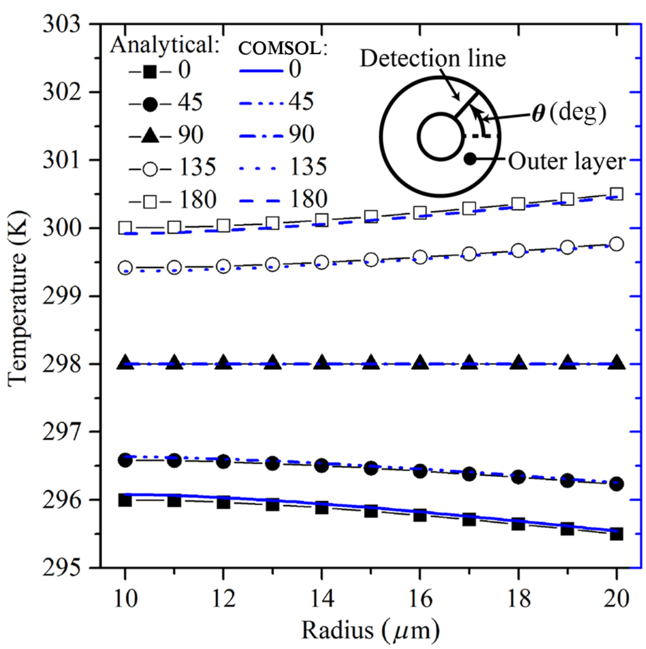

FIG. 6. Comparison of temperature distribution in outer layer.

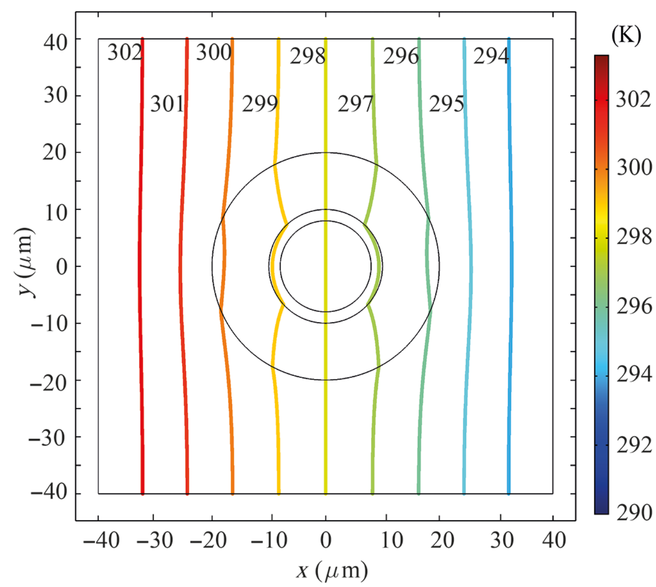

FIG. 8. Isotherms corresponding to reduced effective conductivities.

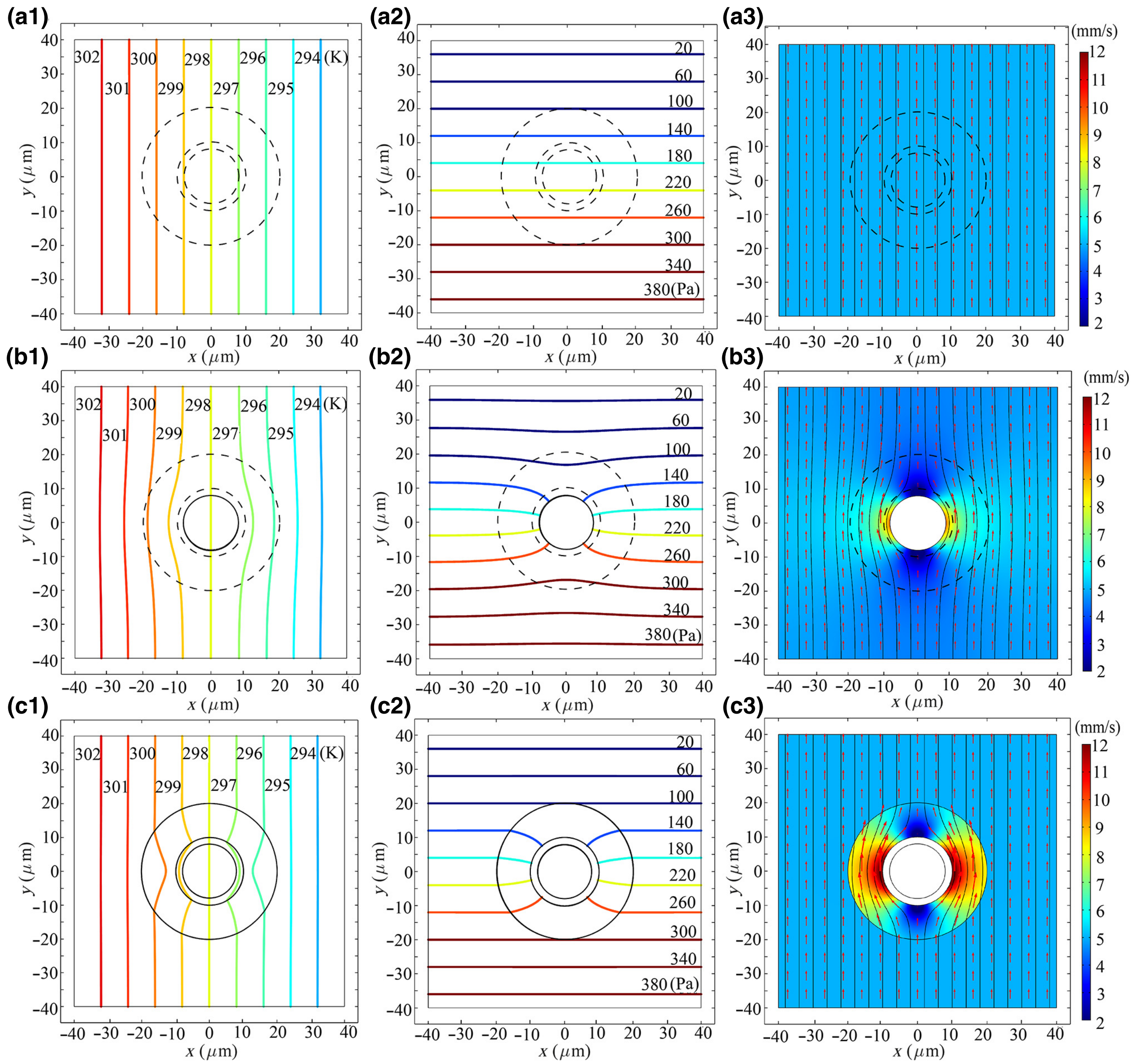

FIG. 9. Simulation results. (a) Bare background without obstacle and cloak. (b) Background with obstacle only. (c) Background with obstacle and bilayer cloak. The first, second, and third panels of each row represent isotherms, isobars, and fluid velocity (streamlines), respectively.

comparison for temperature and pressure distribution in the outer porous layer, respectively. Very good agreement is obtained. The slight difference in the temperature comparison (Fig. 6) is because the inner layer in the COMSOL simulation is not perfectly insulated.

A sensitivity calculation is conducted to illustrate the limitation of the assumption concerning conduction being dominant over convection in the background and outer layer. The effective conductivity of the background is reduced by 10 times to 1 W/m K (hence the outer-layer conductivity becomes 1.67 W/m K), resulting in a Péclet number of approximately 0.3. Figure 8 shows the isotherms in the background and outer layer. It can be seen that the isotherms in the background visually deviate from the vertical, implying that the temperature distribution is not precisely linear as the conduction equation requires. Since COMSOL solves the full advection-diffusion equation in the background and the outer layer for the porous medium, the advection term in this case is not negligible and our bilayer model becomes invalid. This sensitivity case gives some indication of the order of magnitude of the Péclet number to which our model applies.

To better visualize the performance of our bilayer convection cloak, we perform additional COMSOL calculations, for the same parameters as considered in the analytical solutions (Sec. III), for the following configurations: a bare background configuration without the obstacle (i.e., cloaked region) or cloak and a reference configuration with only the obstacle (and without cloak). Figure 9 shows the simulation results. For the bare background (first row in Fig. 9) with neither the obstacle nor cloak, the background temperature and pressure field are linearly varying, and the velocity is uniform in the *y* direction as specified. Once the obstacle to be cloaked is embedded in the background, it disturbs the thermal and hydrodynamic fields as indicated (second row in Fig. 9). When the bilayer cloak is wrapped around the obstacle, the background thermal and hydrodynamic fields are not impacted, demonstrating the functionality of the proposed bilayer cloak in controlling both fluid and thermal fields.

V. CONCLUSIONS

In conclusion, a bilayer convection cloak capable of controlling simultaneously the thermal and hydrodynamic fields has been proposed and analyzed. For the same physical system as considered in Dai *et al.* [3], which is based on transformation thermodynamics and nonhomogeneous anisotropic porous medium, we have shown that a bilayer design using only bulk isotropic materials is possible. The bilayer design uses an inner layer made of impenetrable and perfectly insulated material and a porous outer layer with analytically derived isotropic permeability and effective conductivity. Numerical simulation using practically attainable material properties demonstrates the cloaking function of the proposed cloak, both hydrodynamically and thermally. Also, agreement between analytical and numerical results is excellent, verifying the validity of the major assumptions made in the theoretical derivation.

Additionally, we remark that the hydrodynamic solution, Eq. (28), represents a fully functional hydrodynamic cloak (without any heat transfer) capable of cloaking an external uniform flow field in either the horizontal or vertical direction, provided the background and outer-layer region obey Darcy's law for flow in a porous medium. This is an exact parallel with the conduction cloak based on the bilayer theory, thanks to the analogy between the Fourier law of heat conduction and Darcy's law of flow in porous media.

ACKNOWLEDGMENTS

This study is supported by the Taiwan Ministry of Science and Technology (MOST) under Grants No. MOST-108-2811-E-006-500 (W.-S.Y.) and No. MOST-107-2221-E-006-126-MY3 (R.-J.Y.).

[1] S. Guenneau, C. Amra, and D. Veynante, Transformation thermodynamics: Cloaking and concentrating heat flux, Opt. Express **20**, 8207 (2012).

[2] T. Han, X. Bai, D. Gao, J. T. L. Thong, B. Li, and C. W. Qiu, Experimental Demonstration of a Bilayer Thermal Cloak, Phys. Rev. Lett. **112**, 118 (2014).

[3] S. Dai, J. Shang, and J. Huang, Theory of transformation thermal convection for creeping flow in porous media: Cloaking, concentrating, and camouflage, Phys. Rev. E **97**, 022129 (2018).

[4] S. Dai and J. Huang, A transient regime for transforming thermal convection: Cloaking, concentrating, and rotating creeping flow and heat flux, J. App. Phys. **124**, 235103 (2018).

[5] Y. A. Urzhumov and D. R. Smith, Fluid Flow Control with Transformation Media, Phys. Rev. Lett. **107**, 074501 (2011).

[6] J. Park, J. R. Youn, and Y. S. Song, Hydrodynamic Metamaterial Cloak for Drag-Free Flow, Phys. Rev. Lett. **123**, 074502 (2019).

[7] J. Park, J. R. Youn, and Y. S. Song, Fluid-Flow Rotator Based on Hydrodynamic Metamaterial, Phys. Rev. Appl. **12**, 061002 (2019).

[8] Y. A. Urzhumov and D. R. Smith, Flow stabilization with active hydrodynamic cloaks, Phys. Rev. E **86**, 056313 (2012).

[9] D. Culver and Y. Urzhumov, Forced underwater laminar flows with active magnetohydrodynamic metamaterials, Phys. Rev. E **96**, 063107 (2017).

[10] J. Bear, *Modeling Phenomena of Flow and Transport in Porous Media* (Springer International Publishing, Cham, Switzerland, 2018).

[11] M. W. Kays and M. E. Crawford, *Convective Heat and Mass Transfer* (McGram Hill Ryerson, Ltd., New York, USA, 1980).

[12] Supplemental material of [2] available at http://link.aps.org/supplemental/10.1103/physrevlett.112.054302.

[13] K. Arbenz and A. Wohlhauser, *Advanced Mathematics for Practicing Engineers* (Artech House, Norwood, Massachusetts, 1986).